

Electronic Supplementary Information (ESI)

**Design of a novel green bio-based organic-inorganic hybrid material for cost-effective and sustainable monitoring of antibiotic residues**

Guowen Qin,<sup>a</sup> Huilin Song,<sup>a</sup> Dan Wu,<sup>a</sup> Yuqi Zhang,<sup>a</sup> Peiqi Li,<sup>a</sup> Kaidi Zhang,<sup>a</sup> Yang Zheng,<sup>\*b</sup> Shunli Ji<sup>\*a</sup>

<sup>a</sup>*Department of Pharmaceutical Analysis, China Pharmaceutical University, No.24, Tongjiaxiang, Nanjing 210009, China*

<sup>b</sup>*CR Medicon (Nanjing) Biotechnology Co., Ltd, No.18, Zhilan Road, Nanjing, 210009, China.*

\*Corresponding authors

E-mail address: yang.zheng@crmedicon.com (Y. Zheng); 1020162527@cpu.edu.cn (S. Ji).

## Text S1. Experimental

### 1.1 HPLC-MS/MS analysis

An Agilent 1200 Infinity HPLC system coupled with a 6410B triple quadrupole mass spectrometer was used for HPLC-MS/MS analysis (Agilent, USA). The MACs were separated using a XCharge C18 column (100 mm × 2.1 mm, 3 μm, Acchrom, Beijing, China) with a flow rate of 0.3 mL·min<sup>-1</sup> at 30 °C. The injection volume was 5 μL. The binary mobile phases were 0.2% FA in ACN (A) and 0.2% FA in water (B). The gradient elution mode was as follows: 0~0.5 min=90% B; 0.5~8 min=90% B to 42% B; 8~8.5 min=42% B to 90% B; 8.5~16 min=90% B.

The mass spectrometry detection was performed in positive electrospray ionization (ESI<sup>+</sup>) and multiple reaction monitoring (MRM) modes. The optimal parameters were set as follows: capillary voltage (5000 V); drying gas temperature (350 °C); drying gas flow (11 L·min<sup>-1</sup>); nebulizer pressure (45 psi). All of the data was processed and analyzed by Mass Hunter software (Agilent Technology, Palo Alto, CA, vB01.03 and vB01.04).

### 1.2. Adsorption selectivity

The selectivity of SiO<sub>2</sub>@PVA/HA were evaluated towards seven compounds (streptomycin, sulfadiazine, tetracycline, enrofloxacin, difluoxacin, lomefloxacin and pefloxacin). Sample pretreatment and SPE procedures are carried out in accordance with 2.11.

Streptomycin analysis was performed on an Agilent-1200-Infinity HILIC system equipped with a 6410 triple quadrupole electrospray ionization (ESI) MS (Agilent, USA). A Click Xion HILIC column was used (Acchrom Corp., 150 mm long × 3 mm i.d., 5 μm dia.) at 30 °C. The mass spectrometer was operated in the positive ESI mode with the drying gas temperature of 623 °C, nitrogen gas flow at 10 L·min<sup>-1</sup>, nebulizer pressure of 40 psi, and capillary voltage of 4000 V. The mobile phase of gradient elution consisted of H<sub>2</sub>O/FA (99/1, v/v, A) containing 30 mM NH<sub>4</sub>FA, ACN/H<sub>2</sub>O/FA (80/19/1, v/v/v, B) containing 30 mM NH<sub>4</sub>FA. Procedure was 10% A for 1 min followed by a linear increase to 90% A over a 9 min period, then held for 1 min, finally returned to 10% A in 1 min and re-equilibrated for 10 min. The total runtime was 22 min.

Chromatographic analysis of enrofloxacin, difluoxacin, lomefloxacin and pefloxacin (10 μg·mL<sup>-1</sup>) were performed on a HPLC apparatus (Agilent 1100 Infinity, USA) equipped with a diode array detector (DAD). Enrofloxacin, difluoxacin, lomefloxacin and pefloxacin were separated on a XTerra®RP18 (150 mm × 4.6 mm, 5 μm) analysis column and the temperature of the column compartment was maintained at 30 °C. The UV detection wavelength of enrofloxacin, difluoxacin and pefloxacin were performed at 278 nm, while lomefloxacin at 290 nm. The mobile phase was acetonitrile as solvent A and 0.05% phosphoric acid (adjust pH to 3 with TEA) as solvent B at a flow rate of 1.0 mL·min<sup>-1</sup>. A gradient elution program was 0-5 min, A:B (12:88, v/v); 5-9 min, A:B (17:83, v/v); 9-11 min, A:B (17:83, v/v); 11-12 min, A:B (12:88, v/v); 12-17 min, A:B (12:88, v/v).

Chromatographic analysis of sulfadiazine and tetracycline (10 μg·mL<sup>-1</sup>) were performed on a HPLC apparatus (Agilent 1100 Infinity, USA) equipped with a diode array detector (DAD). Sulfadiazine and tetracycline were separated on a XTerra®RP18 (150 mm × 4.6 mm, 5 μm) analysis column and the temperature of the column compartment was maintained at 30 °C. The UV detection wavelength of sulfadiazine was performed at 266 nm, while tetracycline at 280 nm. The mobile phase was acetonitrile as solvent A and 0.1% FA-H<sub>2</sub>O as solvent B at a flow rate of 1.0 mL·min<sup>-1</sup>. A gradient elution program was 0-3 min, A:B (16:84, v/v); 3-7 min, A:B (25:75, v/v); 7-11 min, A:B (16:84, v/v).

### 1.3. Pre-treatment process for enrichment of MACs with HMMIPDAs and HPMIPs

Five milliliters of milk sample were accurately transferred into a 10 mL polypropylene centrifuge tube and fortified with 200 μL of the working solution at an appropriate concentration.<sup>1</sup> After adding 200 μL of 50% w/v trichloroacetic acid solution, the mixture was homogenized thoroughly and centrifuged at 10000 rpm for 2 minutes. Then 2.5 mL of the upper layer extract was accurately transferred into a 5 mL polypropylene centrifuge tube and pH value was adjusted to 7~8 with 2 M sodium hydroxide solution. The solution was centrifuged for another 5 minutes to remove the precipitate formed in the neutralization process, and all of the supernatants was transferred into another 10 mL polypropylene centrifuge tube. Then 10 mg of HMMIPDAs adsorbent were immersed into the milk extract solution and sonicated for 5 minutes to make the nanoparticles contact entirely with the target analytes. Subsequently, the HMMIPDAs adsorbent were isolated by centrifugation for 2 minutes at 10,000 rpm and rinsed with 1 mL of 5% methanol in deionized water to remove possible interferences. Finally, 1 mL of 5% ammonia in methanol was used to elute captured analytes from HMMIPDAs adsorbent by sonicated for about 5 minutes. After desorption, the eluted fractions were evaporated to dryness by N<sub>2</sub> stream and then reconstituted with 200 μL of the mobile phase for HPLC-MS/MS analysis.

Honey samples were selected for the valuation of HPMIPs.<sup>2</sup> Sample preparation was carried out as follow: 2 g of honey was weighed into a capped 15 mL polypropylene centrifuge tube and 10 mL of phosphate buffer (20 mM, pH 8.0) was added. The mixture was vortex-mixing for 30 s, the samples were centrifuged at 4000 rpm for 10 min. The supernatant was then transferred to a clean tube and then 10 mg of HPMIPs were immersed into the honey extract solution and shifted in a thermostatic oscillator for extracting at 25 °C and 200 rpm for 20 min. Subsequently, the HPMIPs were isolated by centrifugation for 2 min at 4000 rpm and rinsed with deionized water (1.0 mL) and acetonitrile (1.0 mL) to remove possible interferences. Finally, 1 mL methanol/ acetic acid (98/2, v/v) was used to elute captured

analytes from HPMIPs by vortexed for about 1 min. After desorption, the eluted fractions were evaporated to dryness by N<sub>2</sub> stream and then reconstituted with 200 μL of the mobile phase for HPLC-MS/MS analysis.

#### 1.4. Preparation of IHA and Fe<sub>3</sub>O<sub>4</sub>@HA materials

IHA were separated by solvent extraction. 5.0 g of HA powder was weighed into a beaker and an appropriate amount of acetone was added. The mixture was stirred thoroughly and sonicated for 15 min. Allow the suspension to stand until most of the particles have settled, centrifuge and separate the supernatant. The above steps were repeated until the supernatant was free of visible particles. The solid precipitates were then freeze-dried to obtain IHA powder and stored under dry and sealed conditions as a sorbent for MACs.

The preparation of HA-grafted magnetic nanoparticles was carried out by two steps, the first is the synthesis of hollow mesoporous amine-functionalized Fe<sub>3</sub>O<sub>4</sub> (Fe<sub>3</sub>O<sub>4</sub>-NH<sub>2</sub>), and the second is the combination of HA and Fe<sub>3</sub>O<sub>4</sub>-NH<sub>2</sub> through amide reaction. Fe<sub>3</sub>O<sub>4</sub>-NH<sub>2</sub> was prepared by one-step solvothermal reaction. Briefly, FeCl<sub>3</sub>·6H<sub>2</sub>O (1.6 g) was the single iron source and dissolved in EG (48 mL). NaOAc (3.2 g) and 1,6-hexanediamine (10.4 g) were added into the EG solution to form a homogeneous solution under a magnetic stirrer. Afterwards, the solution was reacted at 198 °C for 6 h. The black magnetic materials were separated when the mixture cooled down to room temperature and washed several times with EtOH and H<sub>2</sub>O. Finally, the obtained magnetic nanoparticles were dispersed into H<sub>2</sub>O and freeze-dried for 24 h. In order to modify HA on the surface of Fe<sub>3</sub>O<sub>4</sub>-NH<sub>2</sub>, EDC (50 mg) and HA (100 mg) were dispersed in MES buffer (15 mL, 25 mmol·L<sup>-1</sup>, pH 5.6) with magnetic stirring for half an hour, then NHS (30 mg) was added into the solution and kept stirring for quarter of an hour. After that, Fe<sub>3</sub>O<sub>4</sub>-NH<sub>2</sub> (200 mg) previously dispersed in MES buffer (100 mL, 25 mmol·L<sup>-1</sup>, pH 5.6) by ultrasound was added to the solution slowly, and the mixture was stirred for 12 h under mechanical stirrer. Finally, Fe<sub>3</sub>O<sub>4</sub>@HA was collected by a magnet and washed several times with EtOH and H<sub>2</sub>O.

#### 1.5. Application of PVA/SHA as fertilizer

To verify the potential of PVA/SHA as fertilizer, the cabbage was selected as target plant. The abandoned SiO<sub>2</sub>@PVA/HA adsorbent after a plurality repeated application can be divided and recovered by heating in water solution. SiO<sub>2</sub> and IHA obtained by centrifugation continue to be used as the raw materials for the preparation of new adsorbent, and the recovered supernatant consisting of PVA/SHA was further used as compound fertilizer to promote plant growth. Specifically, the soil taken from the same site was divided into equal parts and then added to two identical pots and one of which was used as the control group, and the other was used as the experimental group. Subsequently, the same number of seeds were placed in the control and experimental groups respectively. PVA/SHA solution was added to the experimental group, and the same volume of water was added to the control group. The seed germination and post-germination seedling growth were recorded. The pH of the soil in the two pots was measured on 1:3 (soil: water) using pH meter.

#### Text S2. Theoretical computational analysis

To gain more insight into the interactions between the SiO<sub>2</sub>@PVA/HA and MACs, DFT calculations were performed. Firstly, as adsorbent are intricate mixtures and SiO<sub>2</sub> only acts as the carrier of the adsorbent, the combination of PVA and HA as the model structure, which are the basic components of adsorbent and can reflect the physicochemical properties of the noumena, are used to calculate the combining energies with MACs.<sup>3,4</sup> The optimized structures were utilized to further assess the intermolecular interactions between MACs and SiO<sub>2</sub>@PVA/HA. Fig. S7e showed significant H-bonding interactions between amino groups (-N) of MACs with the oxygen atom of -OH of PVA/HA with the distance range of 2.2-2.5 Å. Other than that, n-π interactions were also observed between the lone pair electrons of oxygen of -OH groups of MACs with π orbitals of aromatic benzene rings of PVA/HA (Fig. S7e). In addition, RGD results show that the interaction between PVA/HA and MACs includes hydrogen bond interaction, electrostatic interaction and hydrophobic interaction (Fig. S7f).

## 2. Results and discussion

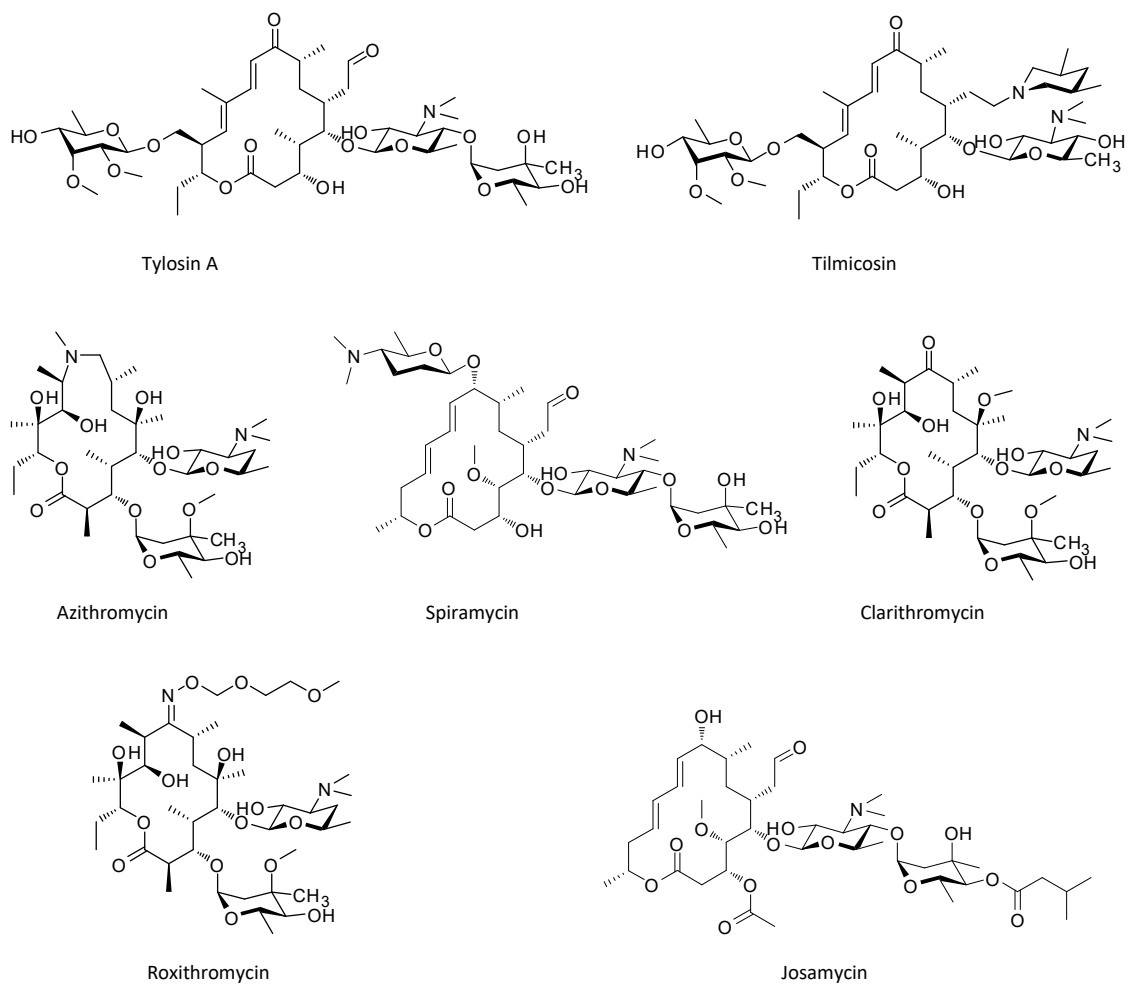


**Fig. S1.** The chemical structures of seven MACs.

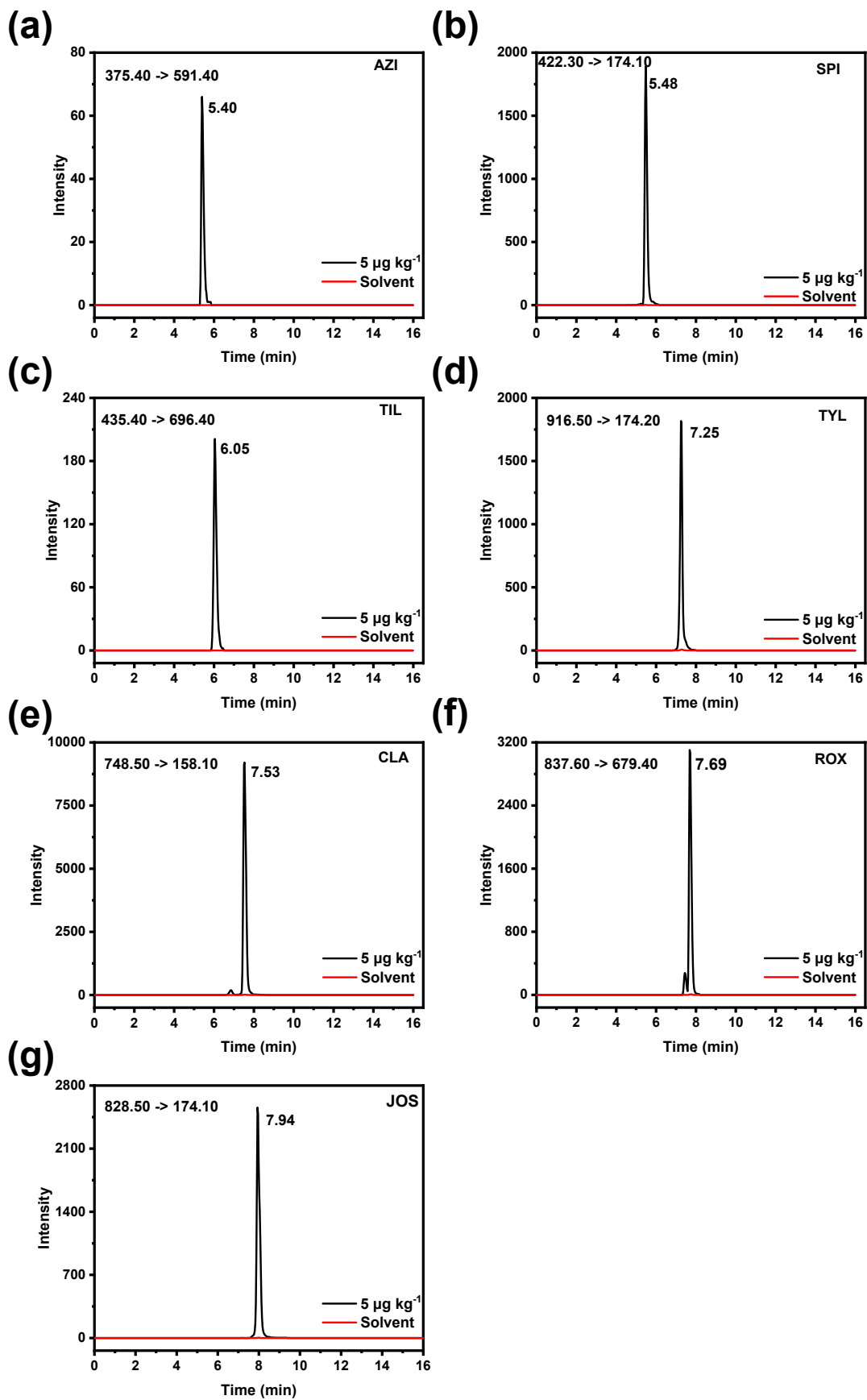
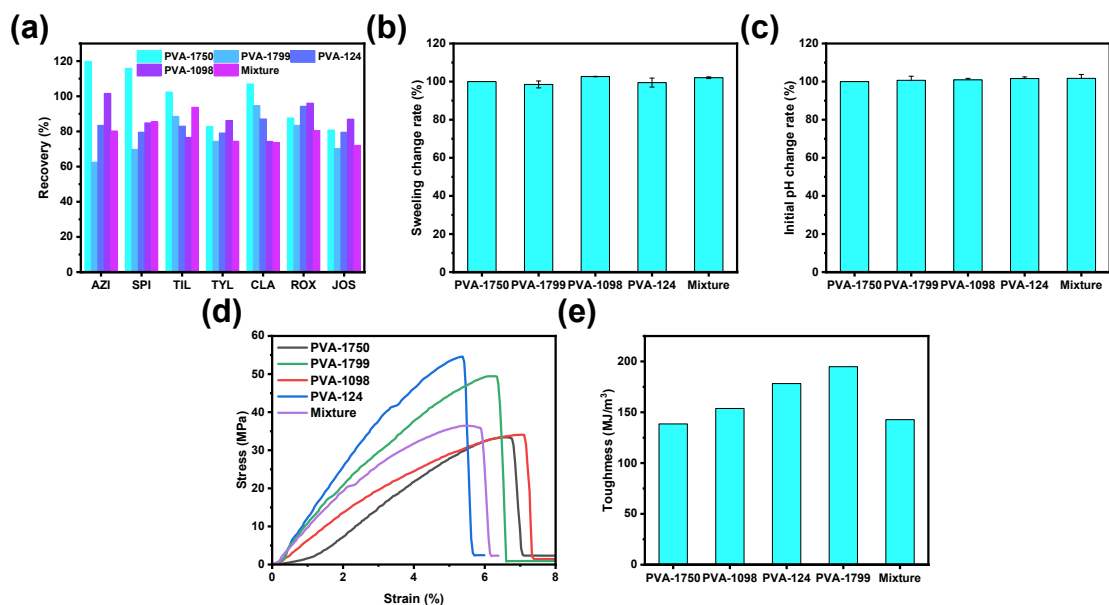
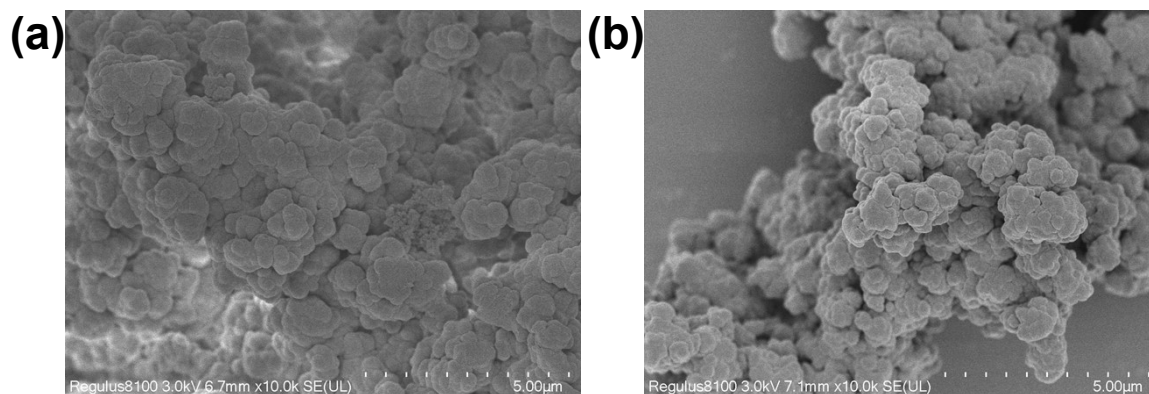


Fig. S2. MRM chromatograms of seven MACs compounds.



**Fig. S3.** (a) Extraction efficiency of adsorbents prepared with different PVA products. (b) Swelling of adsorbents prepared with different PVA products ( $H_2O$  were used to study the swelling property of  $SiO_2@PVA/HA$ ). (c) Initial pH of adsorbents prepared with different PVA products. (d) Stress-strain curves of the different PVA films. (e) Toughness of the different PVA films.



**Fig. S4.** SEM image of HA (a) and IHA (b).

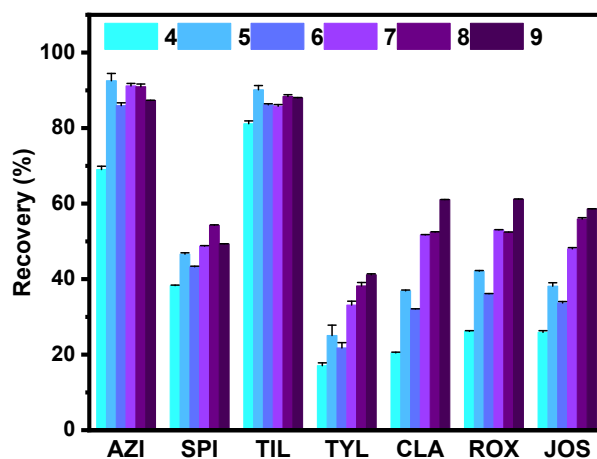


Fig. S5. Effect of pH on the extraction efficiency by IHA adsorbent.

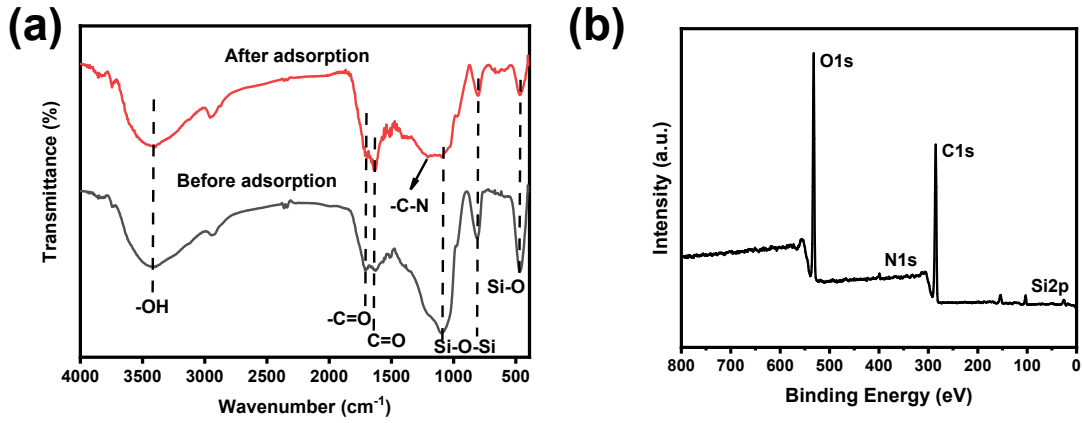
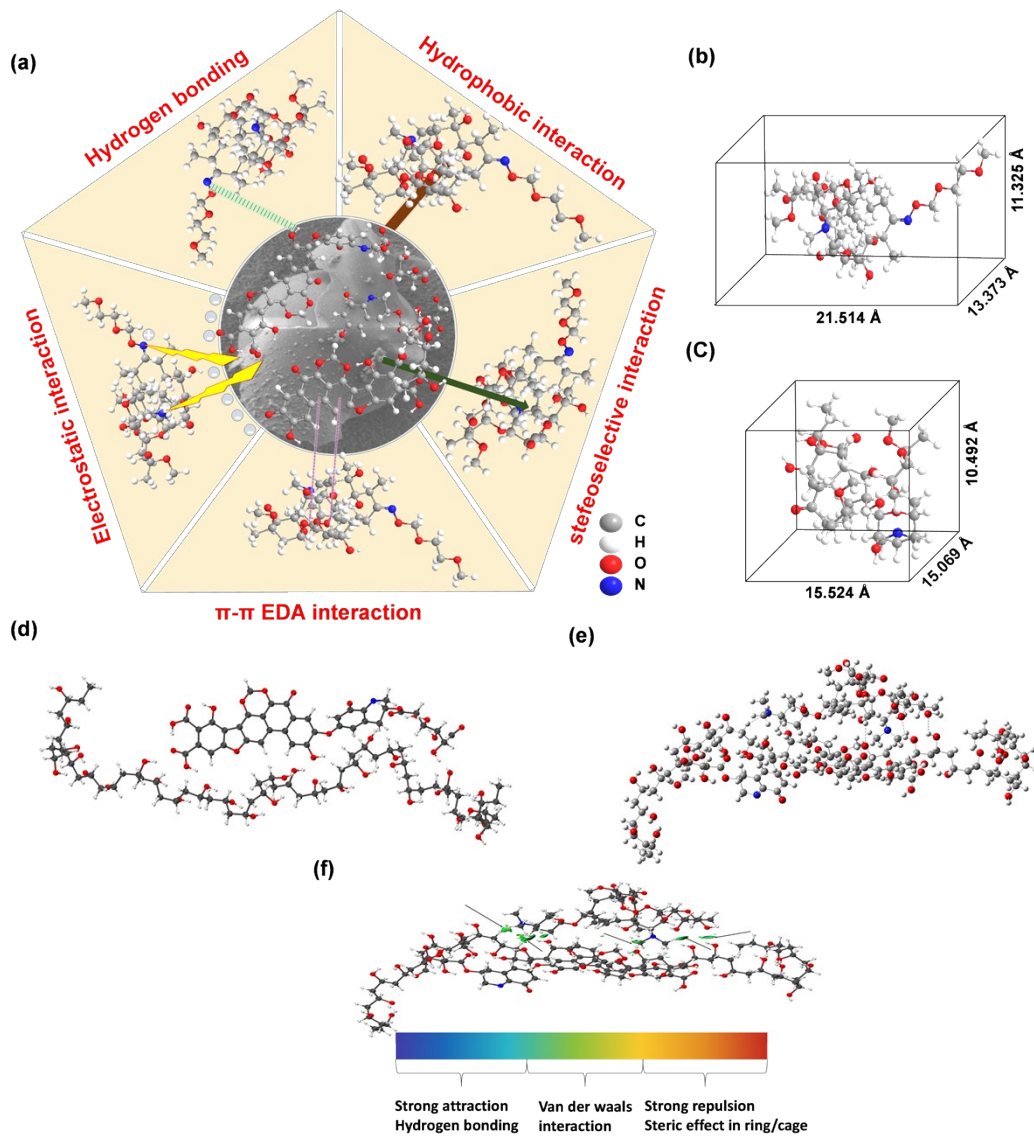
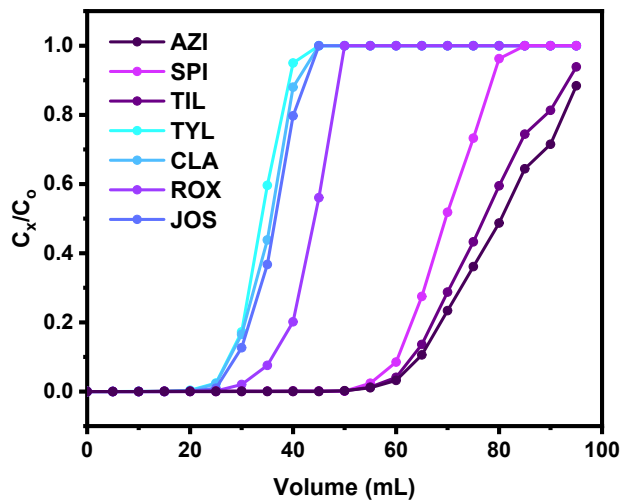


Fig. S6. (a) FT-IR spectra of SiO<sub>2</sub>@PVA/HA before and after SPI adsorption and (b) XPS spectra of SiO<sub>2</sub>@PVA/HA after SPI adsorption.



**Fig. S7.** (a) Adsorption mechanism between the adsorbent and adsorbate. (b) The molecular geometry construction of ROX and (c) CLA. (d) Optimized structures of PVA/HA. (e) Binding path for interaction between PVA/HA and SPI obtained by DFT calculations. (f) Reduced density gradient (RDG) isosurfaces, the color bar indicates the hydrogen bonds (blue), Van der Waals interactions (green), and steric repulsion forces (red).



**Fig. S8.** The breakthrough volumes (2-95 mL) of seven MACs by  $\text{SiO}_2$ @PVA/HA-based SPE cartridge.

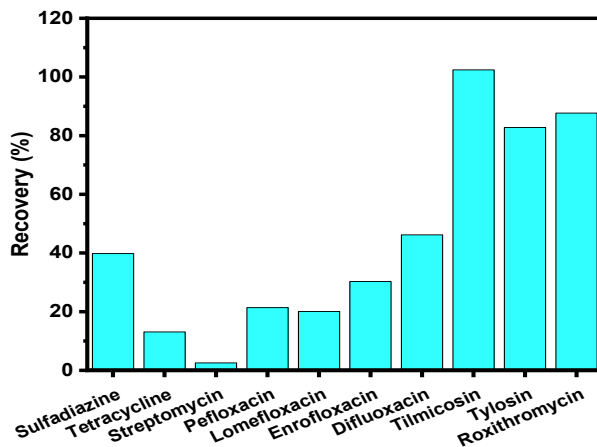


**Fig. S9.** The adsorption performance of MACs and non-MACs on  $\text{SiO}_2$ @PVA/HA at the concentration of  $10 \mu\text{g}\cdot\text{mL}^{-1}$ .

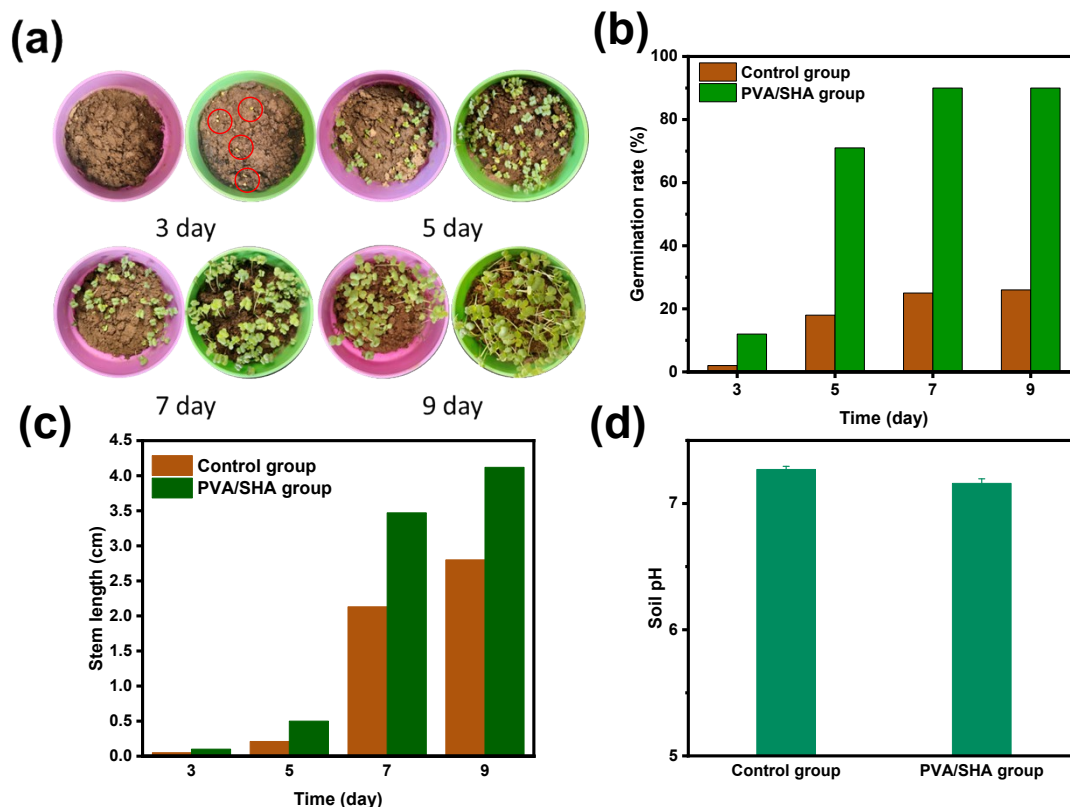


**Fig. S10.** (a) Growth experiment diagram of cabbage (purple pot: control group; green pot: PVA/SHA group). (b) The germination rate and (c) stem length of cabbage in different days. (d) Effects of PVA/SHA on soil pH.

As shown in the Fig. S10a and S10b, a large number of seed germinations were observed on the third day in the experimental group compared to the control group. With the passage of time, the germination rate of cabbage gradually increased and reached equilibrium on the ninth day, the germination rate of the PVA/SHA group was 90%, while the germination rate of the control group was only 26%. Meanwhile, the growth of the seedlings was examined, and as shown in the Fig. S10c, the length of seedlings in the PVA/SHA group was significantly higher than that in the control group. This is mainly due to the fact that PVA/SHA can be used as a carbon source to provide essential nutrients for cabbage, thereby promoting plant growth. In addition, SHA also has the function of improving soil aggregate structure, strengthening soil chelation ability, promoting soil microbial reproduction and water and fertilizer preservation. Although SHA has many effects to improve soil quality, its highly acidic structural characteristics may cause soil acidification, which is detrimental to the growth of most plants. Therefore, the effect of PVA/SHA on soil pH was studied and the results are shown in Fig. S10d. The exciting thing is that, compared to the control group, the soil pH in the experimental group did not change significantly, indicating that the presence of PVA with acid and alkali resistance can effectively prevent soil acidification and make HA play a greater growth-promoting role. Therefore, it can be confirmed by the plant growth experiments that the abandoned adsorbent can be used as a fertilizer in agriculture.

**Table S1.** The properties of MACs

Analytes	pKa		Log P	Log D (pH=3)	Log D (pH=9)	Chemical formula	CAS number
AZI	9.57	8.91	2.44	-4.56	1.55	C <sub>38</sub> H <sub>72</sub> N <sub>2</sub> O <sub>12</sub>	83905-01-5
SPI	9.33	8.44	2.50	-4.50	1.92	C <sub>43</sub> H <sub>74</sub> N <sub>2</sub> O <sub>14</sub>	8025-81-8
TIL	10.16	8.55	4.19	-2.81	2.87	C <sub>46</sub> H <sub>80</sub> N <sub>2</sub> O <sub>13</sub>	108050-54-0
TYL	8.43	/	2.32	-1.18	2.21	C <sub>46</sub> H <sub>77</sub> NO <sub>17</sub>	1401-69-0
CLA	9.00	/	3.24	-0.26	2.94	C <sub>38</sub> H <sub>69</sub> NO <sub>13</sub>	81103-11-9
ROX	9.08	/	3.00	-0.58	2.66	C <sub>41</sub> H <sub>76</sub> N <sub>2</sub> O <sub>15</sub>	80214-83-1
JOS	8.51	/	3.22	-0.28	3.09	C <sub>42</sub> H <sub>69</sub> NO <sub>15</sub>	16846-24-5

Note: This data comes from <https://www.chemaxon.com>.

**Table S2.** The kinetics, isotherm and thermodynamic models used in the adsorption experiment

Model	Equation	Parameters
Langmuir adsorption isotherm	$C_e/Q_e = 1/K_L Q_m + C_e/Q_m$	<p><math>Q_e</math>=amount of SPI adsorbed at equilibrium (mg·g<sup>-1</sup>)</p> <p><math>C_e</math>=SPI concentration of solution at equilibrium (mg·L<sup>-1</sup>)</p> <p><math>Q_m</math>=maximum adsorbed capacity (mg·g<sup>-1</sup>)</p> <p><math>K_L</math>=Langmuir adsorption isotherm constant (L·mg<sup>-1</sup>)</p>
Freundlich adsorption isotherm	$\ln q_e = \ln K_F + (\ln C_e)/n$	<p><math>K_F</math>=Freundlich adsorption coefficient (mg<sup>1-n</sup>·g<sup>-1</sup>·L<sup>-n</sup>)</p> <p><math>n</math>=Freundlich index</p>
Pseudo-first-order kinetic	$Q_t = Q_e(1 - \exp(-K_1 t))$	<p><math>Q_t</math>=amount of SPI adsorbed at any time t (mg·g<sup>-1</sup>)</p> <p><math>Q_e</math>=amount of SPI adsorbed at equilibrium (mg·g<sup>-1</sup>)</p>
Pseudo-second-order kinetic	$Q_t = (k_2 Q_e^2 t) / (1 + k_2 Q_e t)$	<p><math>K_1</math>=pseudo-first-order rate constant (g·mg<sup>-1</sup>·min<sup>-1</sup>)</p> <p><math>K_2</math>=pseudo-second-order rate constant (g·mg<sup>-1</sup>·min<sup>-1</sup>)</p>
Thermodynamic parameters	$\Delta G = -RT \ln K_D$ $\Delta G = \Delta H - T \Delta S$ $K_D = q_e / c_e$	<p><math>\Delta G</math>=Gibbs free energy change (kJ·mol<sup>-1</sup>)</p> <p><math>\Delta S</math>=entropy change (J·mol<sup>-1</sup>·K<sup>-1</sup>)</p> <p><math>\Delta H</math>=enthalpy change (kJ·mol<sup>-1</sup>)</p> <p><math>R</math>=the gas constant (J·mol<sup>-1</sup>·K<sup>-1</sup>)</p> <p><math>T</math>=the absolute temperature (K)</p> <p><math>K_D</math>=the equilibrium constant</p>

**Table S3.** Mass spectral parameters of MACs

Analytes	Molecular mass	Precursor Ion (m/z)	Product Ion (m/z)	Fragmentor (V)	Collision Energy (eV)
AZI	749.00	375.4	591.4	115	10
SPI	843.07	422.3	174.1	110	15
TIL	869.15	435.4	696.4	115	15
TYL	916.11	916.5	174.2	150	55
CLA	747.96	748.5	158.1	150	30
ROX	837.06	837.6	679.4	160	15
JOS	828.01	828.5	174.1	160	35

**Table S4.** Physical properties of PVA products

	Alcoholysis Degrees	Molecular weights	Polymerization degree	Price (¥/g)
PVA-1750	50%	~110000	1700	0.056
PVA-1799	99%	~76000	1700	0.136
PVA-124	98-99%	~195000	2400-2500	1.196
PVA-1098	98.0-98.8%	~61000	1400	2.776

**Table S5.** Swelling ratio of SiO<sub>2</sub>@PVA and SiO<sub>2</sub>@PVA/HA

Solvent	SiO <sub>2</sub> @PVA			SiO <sub>2</sub> @PVA/HA		
	W <sub>0</sub> (mg)	W (mg)	Swelling ratio	W <sub>0</sub> (mg)	W (mg)	Swelling ratio
H <sub>2</sub> O	1442.96	1511.38	0.57	1540.23	1786.74	2.05
ACN	1447.68	1470.92	0.19	1534.47	1682.75	1.24
MeOH	1425.67	1442.69	0.14	1541.96	1686.75	1.21

**Table S6.** Adsorption isotherm parameters based on Langmuir and Freundlich models

Isotherm models	Parameters	25 °C	40 °C
Langmuir	Q <sub>m</sub> (mg·g <sup>-1</sup> )	228.31	102.35
	K <sub>L</sub> (L·mg <sup>-1</sup> )	0.0035	0.0044
	R <sup>2</sup>	0.8754	0.9689
	R <sub>L</sub>	0.2632-0.7407	0.2212-0.6944
Freundlich	K <sub>F</sub> (mg <sup>1-n</sup> ·g <sup>-1</sup> ·L <sup>n</sup> )	3.715	2.724
	1/n	0.5917	0.5227
	R <sup>2</sup>	0.9748	0.9843

**Table S7.** The fitting parameters of adsorption kinetics model

	pseudo-first-order			pseudo-second-order		
	Q <sub>e</sub> (mg·g <sup>-1</sup> )	K <sub>1</sub> (min <sup>-1</sup> )	R <sup>2</sup>	Q <sub>e</sub> (mg·g <sup>-1</sup> )	K <sub>2</sub> (g·mg <sup>-1</sup> ·min <sup>-1</sup> )	R <sup>2</sup>
SiO <sub>2</sub> @HA/PVA	32.45	2.385	0.9862	33.13	0.1245	0.9938

**Table S8.** Thermodynamic parameters for SPI adsorption onto SiO<sub>2</sub>@PVA/HA

T (°C)	ΔG (kJ·mol <sup>-1</sup> )	ΔH (kJ·mol <sup>-1</sup> )	ΔS (kJ mol <sup>-1</sup> ·K <sup>-1</sup> )
25	-16.41	-34.16	-0.06
40	-15.51		

**Table S9.** Molecular 3D dimensions of MACs.

	<b>Molecular 3D dimensions (Å)</b>	<b>Arithmetic mean radius (Å )</b>	<b>Geometric mean radius (Å)</b>	<b>Minimum distance from centre (Å )</b>	<b>Maximum distance from centre (Å )</b>	<b>Average distance from centre (Å )</b>
AZI	16.002×15.417×9.978	6.899	6.751	1.932	8.758	6.084
SPI	20.194×14.252×11.820	7.711	7.520	2.289	11.243	6.478
TIL	19.194×13.181×11.337	7.285	7.104	2.794	10.062	6.464
TYL	19.868×12.861×11.120	7.308	7.082	1.373	10.363	6.297
CLA	15.524×15.069×10.492	6.848	6.745	2.455	8.798	6.017
ROX	21.514×13.373×11.325	7.702	7.412	2.666	13.986	6.174
JOS	20.588×15.227×12.105	7.987	7.799	2.333	11.739	6.789
Streptomycin	14.409×10.319×9.580	5.718	5.626	1.729	7.742	5.053
Sulfadiazine	11.714×8.974×5.938	4.438	4.273	2.864	6.597	4.548
Tetracycline	14.773×9.854×6.543	5.195	4.920	2.845	7.927	5.234
Enrofloxacin	16.901×9.997×6.663	5.593	5.201	2.478	9.289	5.751
Difluoxacin	16.160×11.815×6.558	5.756	5.389	2.326	8.827	5.534
Lomefloxacin	15.281×8.525×7.349	5.193	4.928	2.541	7.991	5.535
Pefloxacin	16.262×8.577×6.151	5.165	4.751	2.664	8.611	5.583

**Table S10.** Spiking recoveries, precision and ME of seven MACs in sample

Analytes	Added ( $\mu\text{g}\cdot\text{kg}^{-1}$ )	Honey			Milk			Egg		
		Intra-day n=6 (%)	Inter-day n=3 (%)	ME (%)	Intra-day n=6 (%)	Inter-day n=3 (%)	ME (%)	Intra-day n=6 (%)	Inter-day n=3 (%)	ME (%)
AZI	5	103.2±11.8	97.7±8.9	105.5	97.2±14.5	100.6±9.2	84.2	92.2±9.3	108.1±9.8	81.4
	50	86.2±5.0	89.4±6.6	92.4	92.5±14.0	98.6±3.6	95.2	99.5±6.0	107.6±8.1	82.0
	100	105.1±5.5	83.6±2.0	89.8	96.5±7.6	99.5±4.2	89.9	99.1±4.6	102.4±10.9	89.4
SPI	5	94.2±1.2	98.7±3.6	86.8	96.5±10.7	98.2±12.1	100.7	99.3±13.5	103.5±8.9	82.3
	50	84.3±6.4	86.4±7.5	95.2	91.4±6.8	95.7±3.6	92.0	102.1±5.4	101.4±5.3	84.2
	100	102.6±2.7	83.2±6.9	101.6	96.6±8.8	99.1±3.3	84.1	97.4±5.5	104.8±5.1	98.9
TIL	5	101.8±5.3	93.6±9.6	83.2	101.63±13.5	103.9±11.5	88.0	100.7±10.7	117.9±5.5	110.9
	50	83.4±1.6	80.5±5.5	94.5	96.8±11.2	105.6±6.2	99.9	104.3±8.7	108.1±7.8	97.7
	100	98.8±1.4	83.5±3.0	90.4	97.2±6.0	100.0±2.5	93.5	97.5±4.9	102.8±2.0	89.5
TYL	5	86.7±5.5	104.8±6.5	114.1	107.2±6.5	99.2±12.3	117.4	112.3±7.6	106.0 ±2.8	95.3
	50	89.9±5.9	88.0±9.9	116.0	99.1±6.6	100.2±3.7	91.6	91.3±7.3	97.4±3.3	100.6
	100	88.7±2.7	92.9±8.9	118.1	102.3±8.9	103.2±10.5	98.1	96.5±7.4	109.3±9.3	96.4
CLA	5	85.9±5.0	96.2±2.1	102.5	96.6±4.7	100.9±4.8	104.6	107.8±7.5	100.2±3.0	90.3
	50	89.2±4.8	96.0±6.6	107.7	94.6±6.2	102.5±1.8	107.2	99.4±10.3	97.4±5.5	114.2
	100	91.4±2.7	92.8±7.5	104.0	102.5±13.4	100.4±3.4	83.3	103.6±7.0	104.0±5.6	91.3
ROX	5	94.4±3.6	97.9±6.9	109.6	103.7±6.9	100.4±5.3	107.1	110.0±7.8	102.5±9.2	102.1
	50	103.5±3.9	105.4±6.5	115.5	95.2±6.6	103.0±2.3	111.6	99.9±7.0	98.0±3.8	118.3
	100	104.2±3.2	108.9±5.4	116.3	103.0±4.7	100.2±4.0	96.8	98.4±6.9	106.0±4.4	100.6
JOS	5	97.7±5.7	103.6±3.3	95.9	106.9±7.2	105.3±10.1	115.6	103.8±10.8	94.9±12.6	96.3
	50	98.4±8.0	91.1±7.0	95.5	96.0±8.8	86.6±13.5	93.4	94.3±6.9	99.3±5.7	108.1
	100	95.8±6.7	96.3±6.0	104.7	108.3±5.5	102.6±8.6	82.6	102.5±8.7	111.9±5.4	86.5

**Table S11.** Analytical results of real samples

	<b>AZI</b>	<b>SPI</b>	<b>TIL</b>	<b>TYL</b>	<b>CLA</b>	<b>ROX</b>	<b>JOS</b>
Honey 1	n.d.						
Honey 2	n.d.						
Honey 3	n.d.						
Milk 1	n.d.						
Milk 2	n.d.						
Milk 3	n.d.	n.d.	n.d.	<LOQ	n.d.	n.d.	n.d.
Egg 1	n.d.	n.d.	<LOQ	n.d.	n.d.	n.d.	n.d.
Egg 2	n.d.						
n.d.:			no				detect.

**Table S12.** Comparison of this method with previously reported methods for the determination of MACs

Sample	Target Analytes	Linearity Range	LOQ	Extraction Solvent	Elution Solvent	Pretreatment Technique	Adsorbent	Environmental-friendly	References
Milk	16 MACs and 4 metabolites	1~1000 ng·mL <sup>-1</sup>	1.1~4.0 µg·kg <sup>-1</sup>	ACN 15 mL	N/A	QuEChERS	MgSO <sub>4</sub> and Na <sub>2</sub> SO <sub>4</sub>	YES	5
Muscle	6 MACs	0.1~100 µg·kg <sup>-1</sup>	2.0~5.0 µg·kg <sup>-1</sup>	ACN 5 mL	NH <sub>3</sub> ·H <sub>2</sub> O-MeOH 1mL	MIP	MIMC	NO	6
Chicken	6 MACs	2.5~100 µg·kg <sup>-1</sup> (TYL, TIL, KIT) 1~40 µg·kg <sup>-1</sup> (AZI, CLA)	1.8 µg·kg <sup>-1</sup> (TYL, TIL, KIT) 0.8 µg·kg <sup>-1</sup> (AZI, CLA)	EDTA 0.2 mL and MeOH/ACN 10 mL	NH <sub>3</sub> ·H <sub>2</sub> O-MeOH 5mL	SPE	PAF-6	NO	7
Muscles	10 MACs	0.1~200 µg·kg <sup>-1</sup>	0.3~1.0 µg·kg <sup>-1</sup>	Sodium borate buffer solution 5 mL and EA 5 mL	NH <sub>3</sub> ·H <sub>2</sub> O-MeOH 5mL	MIP	MISPE	NO	8
Cheese	2 MACs	10~200 ng·g <sup>-1</sup>	10 ng·g <sup>-1</sup>	Mcllvaine buffer 15 mL	ACN 6 mL	SPE	C18	NO	9
Tissues and Egg	11 MACs	1~250 µg·L <sup>-1</sup>	2.0 µg·kg <sup>-1</sup> (Egg) 5.0 µg·kg <sup>-1</sup> (Tissues)	ACN 10 mL, EA/MeOH 10 mL and Hexane 5 mL	N/A	d-SPE	Ni-coated MWCNTs	NO	10
Honey, Milk and Egg	7 MACs	0.5~500 µg·kg <sup>-1</sup>	0.008~0.500µg·kg <sup>-1</sup>	MeOH 5 mL	NH <sub>3</sub> ·H <sub>2</sub> O-MeOH 1mL	SPE	SiO <sub>2</sub> @PVA/HA	YES	This method

**Table S13.** The application of HA as sorbent in the field of extraction.

Sample	Analyte	Extraction method	Adsorbent	Preparation method	Environmental-friendly	References
Edible oils	aflatoxins	DSPE	HA	Soxhlet extraction	No	11
Water	glucocorticoids	SPE	HA-C@silica	Thermally condensed	No	12
Edible oils	Fipronil	SPE	HAS-SiO <sub>2</sub>	/	No	13
Human plasma	Steroid hormones	SPE	HA-C@silica	Thermally condensed	No	14
Vegetable Oils	aflatoxins and benzo(a)pyrene	SPE	HAS-SiO <sub>2</sub>	/	No	15
Honey Milk and Egg	7 MACs	SPE	SiO <sub>2</sub> @PVA/HA	Physical crosslinking	Yes	This work

## References

1. S. Ji, J. Huang, T. Li, X. Luo and F. Zheng, *Nano Select*, 2020, **2**, 328-337.
2. S. Ji, T. Li, W. Yang, C. Shu, D. Li, Y. Wang and L. Ding, *Microchim. Acta*, 2018, **185**, 203-212.
3. M. Tanzifi, M. Tavakkoli Yarak, Z. Beiramzadeh, L. Heidarpoor Saremi, M. Najafifard, H. Moradi, M. Mansouri, M. Karami and H. Bazgir, *Chemosphere*, 2020, **255**, 127052-127065.
4. J. El Gaayda, F. Ezzahra Titchou, R. Oukhrib, I. Karmal, H. Abou Oualid, A. Berisha, H. Zazou, C. Swanson, M. Hamdani and R. Ait Akbour, *Separation and Purification Technology*, 2022, **288**, 120607-120624.
5. W. Zhou, Y. Ling, T. Liu, Y. Zhang, J. Li, H. Li, W. Wu, S. Jiang, F. Feng, F. Yuan and F. Zhang, *J. Chromatogr. B*, 2017, **1061-1062**, 411-420.
6. X. Song, T. Zhou, J. Zhang, Y. Su, H. Zhou and L. He, *Polymers*, 2019, **11**, 1109-1124.
7. C. Lan, D. Yin, Z. Yang, W. Zhao, Y. Chen, W. Zhang and S. Zhang, *J. Anal. Methods Chem.*, 2019, **2019**, 1-13.
8. X. Song, T. Zhou, Q. Liu, M. Zhang, C. Meng, J. Li and L. He, *Food Chem.*, 2016, **208**, 169-176.
9. E. L. McClure and C. S. Wong, *J. Chromatogr. B*, 2007, **1169**, 53-62.
10. J. Du, X. Li, L. Tian, J. Li, C. Wang, D. Ye, L. Zhao, S. Liu, J. Xu and X. Xia, *Food Chem.*, 2021, **365**, 130502-130512.
11. P. Liu, Y.-H. Liao, H.-B. Zheng and Y. Tang, *Analytical Methods*, 2020, **12**, 2308-2316.
12. A. Speltini, F. Merlo, F. Maraschi, M. Sturini, M. Contini, N. Calisi and A. Profumo, *Journal of Chromatography A*, 2018, **1540**, 38-46.
13. X. T. Peng, Y. N. Li, H. Xia, L. J. Peng and Y. Q. Feng, *Journal of Separation Science*, 2016, **39**, 2196-2203.
14. A. Speltini, F. Merlo, F. Maraschi, L. Villani and A. Profumo, *Talanta*, 2021, **221**, 121496-121503.
15. F. M. a. P. L. Di Yuan, Liangxiao Zhang, *Toxins*, 2022, **14**, 352-365.